XV Workshop on Physics of Nuclear Fission

Obninsk, 3-6 October, 2000

Analysis of Spallation Residues within the Intranuclear Cascade Model

A. V. Ignatyuk, N. T. Kulagin, V. P. Lunev
Institute of Physics and Power Engineering, 249020 Obninsk, Russia

K.-H. Schmidt
GSI, D-64291 Darmstadt, Germany

Spallation residues produced in liquid hydrogen and deuterium targets by the projectiles ^{208}Pb and ^{238}U with energies of 1 GeV per nucleon have been studied recently at the Fragment-Separator facility at GSI. These data allow to test different versions of the intranuclear-cascade model with much higher accuracy than before. Main contradictions between widely used versions are briefly discussed. The modifications of the models, required to describe the experimental data, are demonstrated.

Introduction

Spallation reactions have recently attracted an increasing interest due to their applications as intense neutron sources for accelerator-driven subcritical reactors or spallation neutron sources [1]. Designs of an accelerator-driven system (ADS) require precise knowledge of nuclide production cross sections in order to be able to predict the amount of radioactive isotopes produced inside the spallation target. Indeed, short-lived isotopes may be responsible for maintenance problems and long-lived ones will increase the long-term radiotoxicity of the system. Data concerning lead are particularly important since in most of the ADS concepts actually discussed, lead or lead-bismuth alloy is considered as the advanced coolant of spallation targets.
The recent experiments, performed at GSI using inverse kinematics, were able to supply the identification of all the isotopes produced in spallation and fission reactions [2-5]. The data obtained can be considered as a crucial benchmark for the theoretical and phenomenological models used in the ADS technology. The precision of these models to estimate residue production cross sections is still far from the accuracy required for technical applications, as it was shown in Refs. [6, 7]. So, in present work we want to discuss the modifications of the Intranuclear Cascade Model (INCM) that are required to reduce the deviations from experimental data.

Main ingredients of INCM

Spallation reactions are generally modeled as a two-stage process. In the first stage, the nucleon-nucleon collisions inside the nucleus induce the loss of a few high-energy nucleons and lead to the formation of excited prefragments [8-10]. This process can be continued by a preequilibrium emission of nucleons in some versions of the INCM [11]. In the second stage, the prefragments deexcite by evaporation of light particles or by fission.
For the reaction ^{208}Pb + p (1 GeV) the distributions of prefragments in masses and excitation energies, which arise after a cascade of nucleon-nucleon collisions inside the nucleus, are shown in Fig. 1. Calculations are performed with three versions of the INCM, which we want do discuss in the present publication: i) LAHET code [14] with default parameters including the preeqilibrium emission of particles, ii) the GSI code based on the Cugnon model [11,12]

combined with the evaporation model ABLA developed at GSI [15] and iii) CASCADO code related historically to the model [10], but with an essentially modified evaporation approach that takes into account the IPPE experience on the level-density and nuclear-fission analysis [16]. All codes give rather low excitation energies 25-50 MeV for the prefragments close to the projectile and the increase of excitation energies up to the averaged values of <E> = 150-220 MeV for the most probable prefragments with A~200-206. Prefragments with higher excitations arise in the mass region A<200 with a relatively low probability. The distributions shown in Fig. 1 can be considered as the input data for the second evaporation stage of the INC.

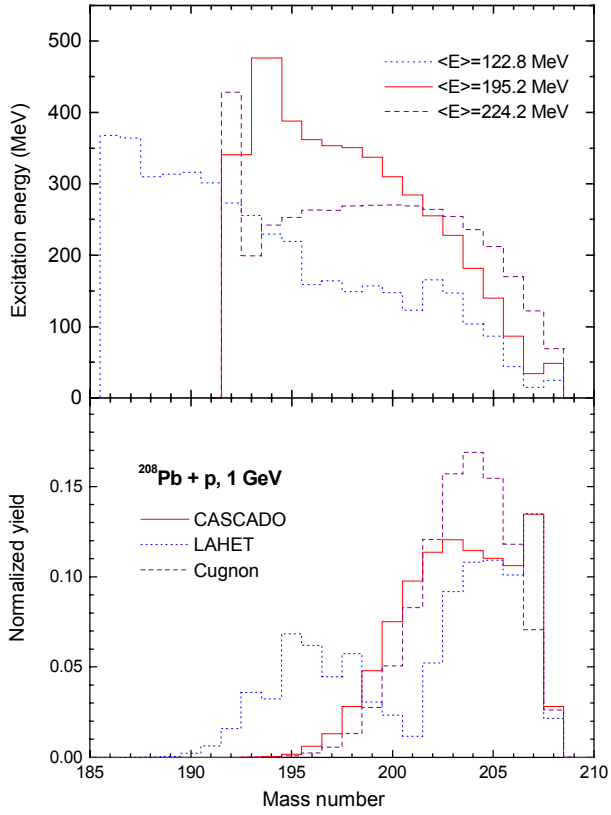

Fig. 1. Distribution of the prefragment masses and excitation energies after the first stage of the INC.

All evaporation models are based on the well-known Weisskopf-Ewing formula for the emission widths [17]

$$\Gamma_i(U) = \frac{(2s+1)m_i \int_0^{U-B_i} \varepsilon \sigma_i(\varepsilon) \rho_i(U - B_i - \varepsilon) d\varepsilon}{\pi^2 \hbar^3 \rho_c(U)} , \qquad (1)$$

where s_i and m_i are the spin and mass of the emitted particle, B_i is its binding energy in the compound nucleus with the excitation energy U, σ_i is the absorption cross section for the inverse reaction, ρ_i and ρ_c are the level densities for the residual and compound nucleus, respectively.

A simple approximation for the absorption cross sections is used widely

$$\sigma(\varepsilon) = \begin{cases} 0 & \text{for } \varepsilon < C_{Coul} \\ \pi R_0^2 & \text{for } \varepsilon \geq C_{Coul} \end{cases} , \qquad (2)$$

where C_{coul} is the height of the Coulomb barrier, which can be defined by the standard formula, and $R_0 = r_0 A^{1/3}$ is the geometrical radius of a nucleus. Within a frame of this approach Eq. (1) can be approximated by the formula

$$\Gamma_i(U) = \frac{(2s+1) m_i r_0^2 A_i^{2/3} T^2 \rho_i(U - B_i - C_i)}{\pi^3 \rho_c(U)} \quad , \tag{3}$$

where T_i is the nuclear temperature for the residual nucleus.

More complex formulas for the emission widths were proposed by Dresner [18], who used the Fermi-gas model relations for the level density in calculations of the integral in Eq. (1) taking into account the exponentially small additional terms connected with the pre-exponential components of the level density formulas. For the excitation energies above the neutron binding energies, that are most important in any practical calculation, the difference between the Dresner description and the calculations based on Eq. (3) seems negligible.

A much more important question for a simple approximation (2) relates to an estimation of the radius parameters r_0 and the Coulomb barriers. With the original formula (1) all calculations can be made on the basis of optical models without any reference to the geometrical cross-section and the effective Coulomb barrier that are required for Eq. (3). The best choice of the parameters r_i, which could differ for different emitted particles, corresponds to the agreement of the results obtained with Eqs.(1) and (3). It is obviously that an exact equality of the two results can be achieved at some energy only. Nevertheless, we could require an agreement between calculations based on Eqs. (1) and (3) at the crucial energies, which correspond to the average energies of the Maxwell spectra of evaporated particles. In the practical versions of the INCM the parameters of the effective Coulomb barriers and the geometrical cross sections are usually estimated from a fit to some experimental data and we should note that the meanings of r_i differ essentially in widely used codes.

Another important component of evaporation models relates to the description of the fission widths. Usually, the well-known Bohr-Wheeler formula [19] is applied for this purpose, which can be written in a slightly simplified form as

$$\Gamma_f^{BW}(U) = \frac{T_f \rho_f(U - B_f)}{2\pi \rho_c(U)} \quad , \tag{4}$$

where B_f is the fission-barrier height.

In the last decades it was recognized that the description of the fission probability for high excitation energies requires some essential modifications of the Bohr-Wheeler approach, which relate to the dynamics of the collective motion. To create a collective mode similar to the fission process, some transient time is required [20]. The dependence of such a time on nuclear properties can be derived from the solution of the time-dependent Fokker-Planck equation for the collective degree of freedom. For a simple harmonic parameterization of the potential of the collective mode, the transient time for the overdamped regime can be estimated by a rather simple expression [20]

$$\tau_f = \frac{\beta}{2\omega^2} \ln \frac{10 B_f}{T_f} \quad , \tag{6}$$

where β is the reduced dissipation coefficient and ω is the corresponding frequency of the approximated harmonic potential.

Taking into account the transient time, the ratio for the fission width can be written in the form

$$\Gamma_f(U) = \Gamma_f^{BW}(U) f_K(\beta) \exp\{-\tau_f \sum_{\nu} \Gamma_\nu(U) / \} \quad , \tag{7}$$

where $f_K = [1+(\beta/2\omega)^2-\beta/2\omega]^{1/2}$ is the Kramers factor [21], responsible for the reduction of the fission probability due to the dissipation, and the sum in Eq. (7) has to be taken over all particle-emission channels that compete with fission. The main effect of the factors, which appear additionally to the Bohr-Wheeler expression, is a hindrance of fission for times smaller than the transient time, and this hindrance reduces strongly the fission widths at excitation energies higher than 100-150 MeV above the fission barrier. It was shown in the analysis of heavy-ion induced reactions, that the hindrance of fission plays a crucial role for the consistent description of the total amount of neutrons and light charged particles emitted by the fissioning nuclei [22], as well as the residual product yields observed in the fragmentation of relativistic heavy ions [23].

The fission barriers that are used in different codes are shown in Fig.2 in comparison with the experimental data available for pre-actinides [16]. It is seen that the considered INCM codes use fission barriers, which differ rather strongly. A simple liquid-drop model is used in LAHET, the Sierk's barriers [24] are applied in the GSI model, and the droplet model fitted to experimental barriers [16] is used in CASCADO. Both the GSI and the CASCADO code take into account the shell corrections to the fission barriers that are very important at excitation energies below 50 MeV for near-magic pre-actinides. The barriers used in LAHET are too low for isotopes between Pt and Pb. It overestimates strongly the fissility of these nuclei and always requires some adjustment of the barriers to obtaine a correct value of the total fission cross sections.

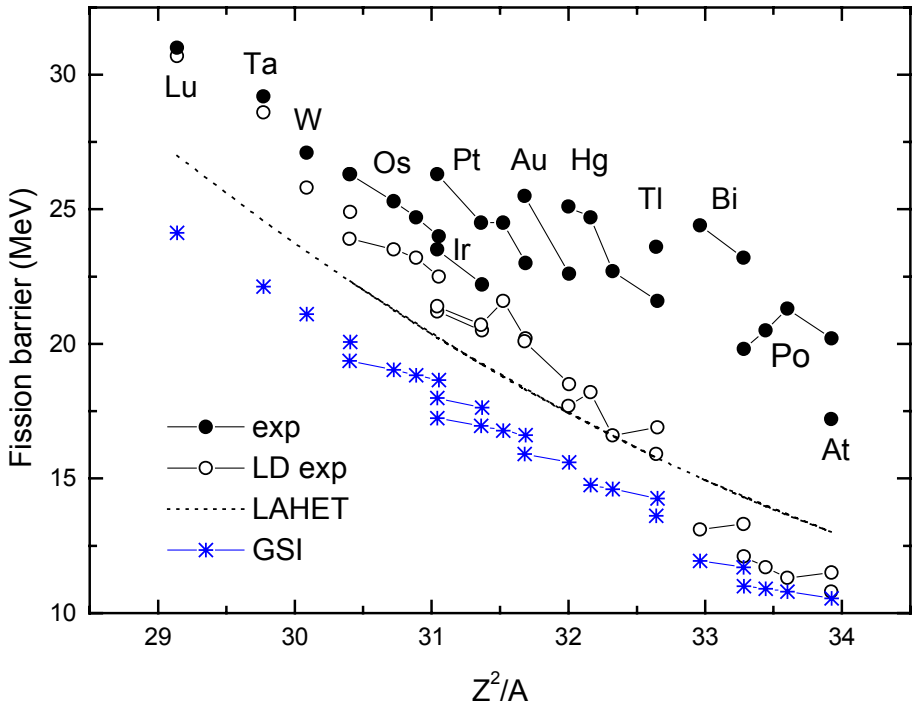

Fig. 2. Experimental fission barriers (solid circles) and the liquid-drop barriers (open circles) as a function of the fissility parameter Z^2/A. The dotted curve shows the fission barriers used in LAHET, and the asterisks represent the liquid drop barriers used in the GSI code.

Comparison with experimental data

The production cross sections of the spallation residues measured at GSI in the reaction of 1 *A* GeV ^{208}Pb with protons [4] are plotted as isotopic distributions in Fig. 3. To avoid too

complex plots, we selected a part of the available experimental data only. Most of the presented distributions exhibit a Gaussian-like shape where the neutron-proton evaporation competition determines the position of the maximum. The produced isotopes populate a corridor between the valley of stability and the proton drip line due to the fact that the excited heavy prefragment evaporates mainly neutrons The most significant deviations from this shape occur for the neutron-rich fragments with masses close to that of the projectile. In the case of these residues only a few neutron-removal channels from low-excited nuclei are responsible for the increased production cross sections.

Calculations performed with different INC plus evaporation-fission models are shown in Fig. 3 together with the corresponding experimental data. The calculations made with the commonly used LAHET code system (Isabel version) [14] gives the isotopic distributions shifted with respect to the experimental ones towards the neutron-rich side. This can be ascribed to the fact that the prediction of the neutron-proton evaporation competition in the Dresner code is not satisfying. On the other hand, in a region very close to the projectile mass LAHET calculations are in good agreement with the data and this result is the direct consequence of a reasonable estimation of the excitation-energy distribution at the end of the INC stage.

The calculations with the Cugnon model (version INCL3 [12]) combined with the GSI evaporation-fission model reproduces much better than the former ones the shape of the experimental isotopic distributions. This comes mainly from a better description of the neutron-proton competition than in the Dresner parameterization [18]. The main defect of the GSI calculations is the underproduction of isotopes very close to the projectile, which represent an important part of the total cross section. This is ascribed to the sharp-surface approximation in the Cugnon model, which leads to a bad description of the most peripheral reactions. These defects result in a poor prediction of the mass distribution, as was demonstrated in complete comparison of the Liège-GSI model calculations with experimental data [3].

The calculations with the CASCADO code, which use for the evaporation-fission model practically the same approximations as the GSI model, differ from the GSI calculations in a mass region close to the projectile. The CASCADO results are close to the LAHET ones for Z=82; that is explained by the similarity of the excitation-energy distributions of the two codes at the end of the INC stage. Differences between the GSI and CASCADO calculations at the low mass region for Z=55 attributes to the fission-fragment contribution, that is, probably, overestimated in the CASCADO results. This question requires a special consideration and the careful analysis of parameters determining the mass distribution of the fission fragments.

We show in Fig. 3 also the results of the empirical parameterization of Silberger et al. [26] for the production cross sections of individual isotopes in high-energy proton interaction, which are widely used in astrophysical applications. It can be seen that the parameterization fails clearly in the prediction of the center-position of isotopic distributions. As it was shown in Ref. [4], the differences between the empirical predictions and the experimental data increase even more for the region of fission fragments.

The calculations with CASCADO for other initial conditions, the reaction of 1 A GeV ^{208}Pb on deuterium, are shown together with preliminary experimental data [5] in Fig. 4. The entrance energy in this case is two times higher than for the hydrogen target, and the corresponding difference arises in the distribution of excitation energies at the end of the INC stage. So, the production cross sections remain approximately the same for Z>70, but they increase by several times for lighter spallation products. The general quality of the theoretical simulation of the experimental data is the same as for the proton case. Some overestimation of calculated yields at the low-mass region can again be attributed to the contribution of the fission fragments.

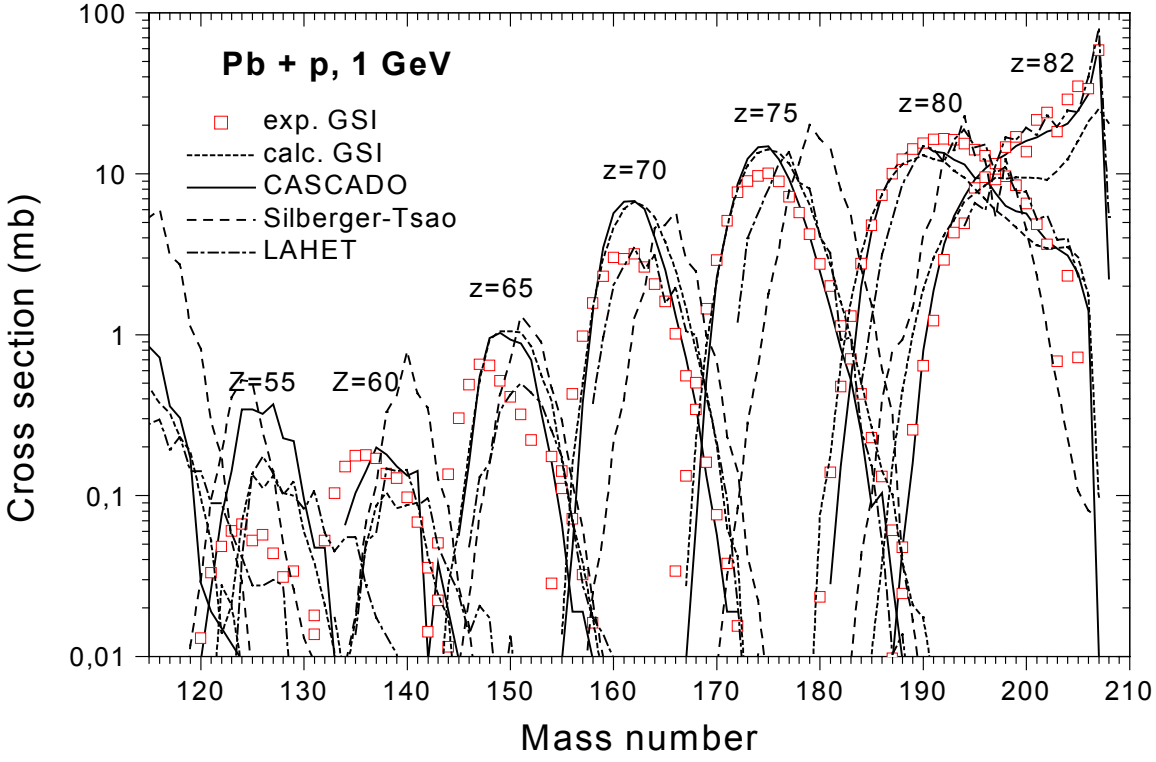

Fig. 3. Experimental data on isotopic distribution of spallation residues in the reaction of 1A GeV ^{208}Pb on hydrogen in a comparison with different versions of INCM calculations and an empirical systematics [26].

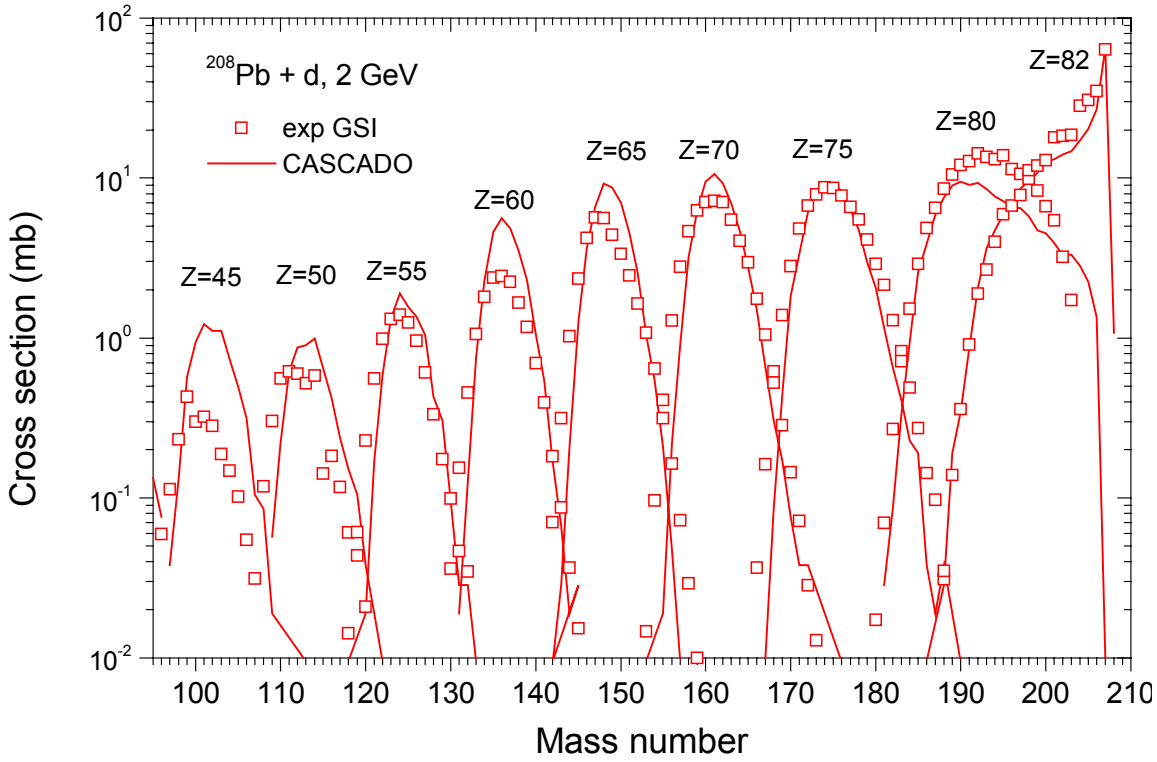

Fig. 4. Preliminary experimental data on isotopic distribution of spallation residues in the reaction of 1A GeV ^{208}Pb on deuterium in a comparison with CASCADO calculations.

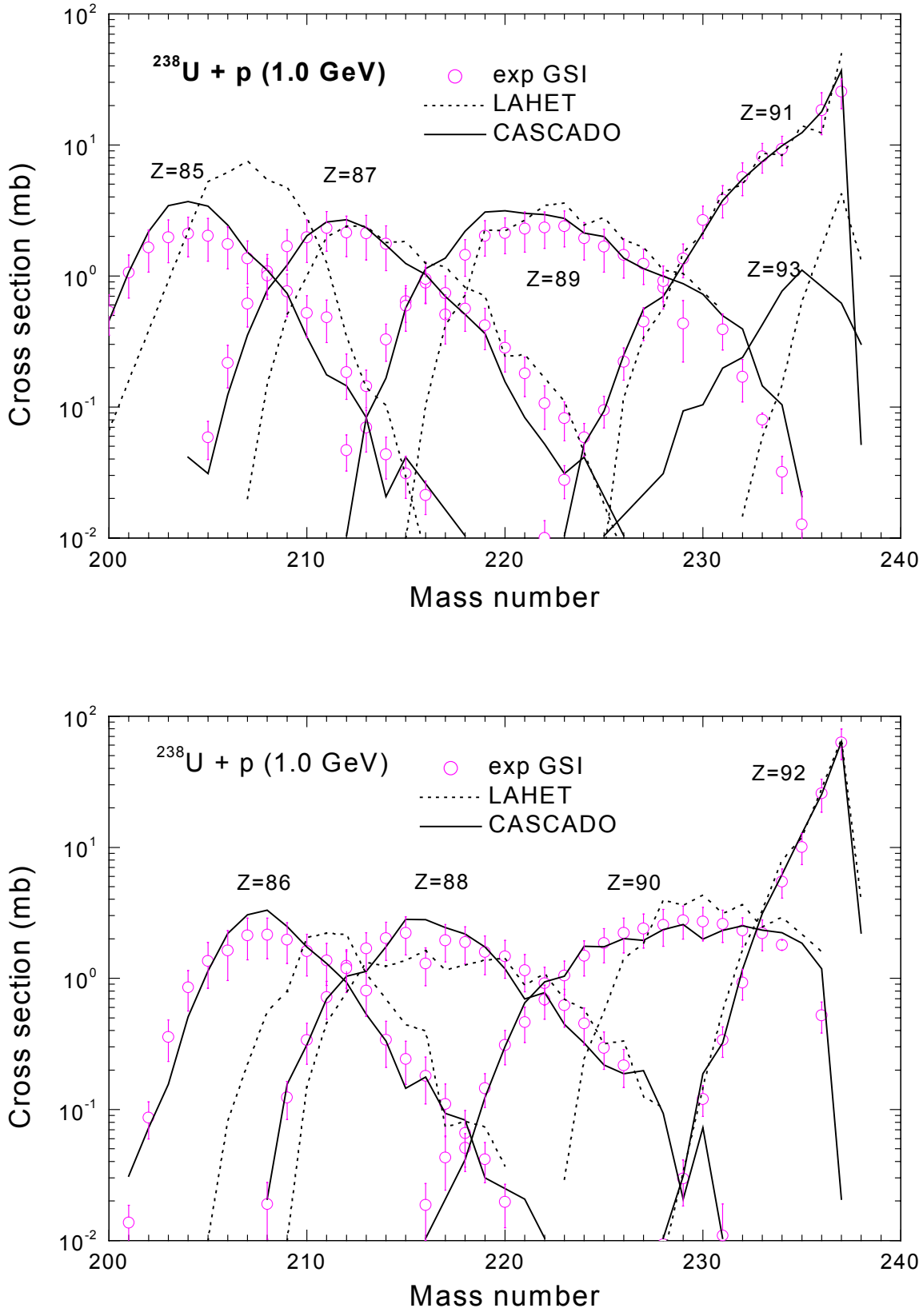

Fig. 5. Preliminary experimental data on isotopic distribution of spallation residues in the reaction of 1A GeV ^{238}U on hydrogen in a comparison with INCM calculations.

In Fig. 5 the results of residual-yield calculations with LAHET and CASCADO are shown together with the corresponding experimental data for the reaction of 1 A GeV ^{238}U on hydrogen [5]. It should to be noted, that for the nuclei with Z>89 the empirical systematics of nuclear fissility (the ratio of the fission width to the neutron one) is used in LAHET, that is based on experimental data for the light charged-particle induced fission at relatively low energies [25]. Such an approach did not take into account any change of the fission widths with the increase of excitation energies. The adopted model well describes the experimental isotopic production cross-sections for Z=92 and a little worse for Z=91, but it comes in contradictions with the experiment for the neutron-deficient isotopes of the elements with Z≤90 (may be excluding Z=88, for which the agreement with the data is much better than for neighbor elements). Because the fission channel is mainly responsible for the deviations of the calculated yields from the experimental ones, an essential improvement of the fission model applied in LAHET is required.
The fission model described above is used in CASCADO for the whole mass region with the fission barriers based on the droplet model with experimental shell corrections. Such corrections are important for residuals close to the projectiles, which have relatively low excitation energies. For prefragments shifted from the projectile more than several mass unites, the liquid-drop component of the fission barriers plays the dominant role. Of course, the hindrance of nuclear fission is important for high excitation energies. Such evaporation-fission model combined with the fast stage of the INC l describes the GSI experimental data for all heavy nuclei with A>200 rather well.
Some results of the CASCADO calculations for lighter fragments were discussed briefly in Ref. [7] in comparison with other versions of INCM and rather scanty experimental data available still recently. The more detailed analysis of the differences between the experimental data and their simulations by various INCM calculations will be justified after the final processing of the whole set of GSI measurements.

Conclusion

The new GSI experimental data on the isotopic distribution of spallation residues of ^{208}Pb and ^{238}U projectiles on hydrogen and deuterium targets were compared with calculations of several frequently used INCM codes. Although none of them provides a detailed description of the experimental data, the improvements of the evaporation-fission model, achieved during the last decades and realized in the Liège-GSI and CASCADO codes, made their results most reasonable for calculations of activities produced in the spallation targets of the designed ADS. Additional adjustment of parameters used by these codes to the whole set of data obtained at GSI could essentially improve the predictive accuracy of current INCM calculations.

References:

1. *Proceedings of the International Conference on Accelerator-Driven Transmutation Technologies and Applications, Las Vegas, 1994*, edited by E. D. Arthur, A. Rodrigues, and S. O. Schriber (AIP Press, Woodbury, NY, 1995).
2. F. Rejmund, B. Mustapha, P. Armbruster, J. Benlliure, M. Bernas, A. Boudard, J. P. Dufour, T. Enqvist, R. Legrain, S. Leray, K.-H. Schmidt, C. Stéphan, J. Taïeb, L. Tassan-Got, and C. Volant, Nucl. Phys. **A 683** (2001) 540.
3. W. Wlazlo, T. Enqvist, J. Benlliure, F. Farget, K.-H. Schmidt, P. Armbruster, M. Bernas, A. Boudard, S. Czajkowski, R. Legrain, B. Mustapha, M. Pravikoff, C. Stephan, J. Taïeb, L. Tassan-Got, and C. Volant, Phys. Rev. Lett. **84** (2000) 5736.

4. T. Enqvist, W. Wlazlo, P. Armbruster, J. Benlliure, M. Bernas, A. Boudard, S. Czajkowski, R. Legrain, S. Leray, B. Mustapha, M. Pravikoff, F. Rejmund, K.-H. Schmidt, C, Stéphan, J. Taïeb, L. Tassan-Got, and C. Volant, Nucl. Phys. **A 686** (2001) 481.
5. T. Enqvist et al., to be published; J. Taïeb, PhD thesis, IPN Orsay, France, 2000.
6. R. Michel and P. Nagel, *International Codes and Model Intercomparison for Intermediate Energy Activation Yields* (OECD_NEA, Paris, 1997).
7. Yu. E. Titarenko, O. V. Shvedov, M. M. Igumnov, S. G. Mashnik, E. I. Karpikhin, V. D. Kazaritsky, V. F. Batyaev, A. B. Koldobsky, V. M. Zhivun, A. N. Sosnin, R. E. Prael, M. B. Chadwick, T. A. Gabriel, and M. Blann, Nucl. Instrum. Methods **A414** (1998) 73.
8. H. W. Bertini, Phys. Rev. **188** (1969) 2227.
9. Y. Yariv and Z. Frankel, Phys. Rev. **C 2**0 (1979) 2227.
10. V. S. Barashenkov and V. D. Toneev, Interaction of high energy particles and nuclei with atomic nuclei, Moscow, Atomizdat, 1972 (in Russian).
11. J. Cugnon, Nucl. Phys. **A462** (1987) 751.
12. J. Cugnon, C. Volant, and S. Vuillier, Nucl. Phys. **A62**0 (1997) 457.
13. S. G. Mashnik, K. K. Gudima and V. D. Toneev, Nucl. Phys. **A401** (1983) 329.
14. R. E. Prael and H. Lichtenstein, Los Alamos Report UR-89-3014, 1989.
15. J.-J. Gaimard and K.-H. Schmidt, Nucl. Phys. **A 531** (1991) 709; A. R. Junghans, M. de Jong, H.-G. Clerc, A. V. Ignatyuk, G. A Kudyaev and K.-H. Schmidt, Nucl. Phys. **A 629** (1998) 635.
16. A. V. Ignatyuk, G. N. Smirenkin, M. G. Itkis et al., Fiz. Elem. Chastits At. Yadra 16 (1985) 709 (Sov. J. Part. Nucl. **16** (1985) 307).
17. V. F. Weisskopf and D. H. Ewing, Phys. Rev. **57** (1940) 935.
18. L. Dresner, Oak Ridge National Laboratory Report ORNL-TM-196, 1962.
19. N. Bohr, J. A. Wheeler, Phys. Rev. **56** (1939) 426.
20. P. Grange, L. Jun-Qing, H. A. Weidenmüller, Phys. Rev. **C 27** (1983) 2063; K. H. Bhatt, P. Grange, B. Hiller. Phys. Rev. **C 33** (1986) 954.
21. H. A. Kramers, Physica **7** (1940) 284.
22. D. Hilscher and H. Rossner*,* Ann. Phys. Fr. **17** (1992) 471.
23. A. V. Ignatyuk, G. A. Kudyaev, A. Junghans, M. de Jong, H.-G. Clerc, K.-H. Schmidt, Nucl. Phys. **A 593** (1995) 519.
24. A. J. Sierk, Phys. Rev. **C 33** (1986) 2039.
25. F. Atchison, in *Proceedings of the Meeting on Targets for Neutron Beam Spallation Sources, Jülich, 1979,* Jül-Conf- 34 (Kernforschungsanlage, Jülich GmbH, 1980).
26. R. Silberberg, C. H. Tsao, and A. F. Barghouty, Astrophys. J. **501** (1998) 911.